at different stages of their life cycles, and initiate developmental changes on encountering each host (*28*). In addition, a variety of marine invertebrates undergo metamorphosis after encountering a particular habitat (*29*). Perhaps mechanisms like those used by *C. elegans* for neuronal control of dauer formation and recovery are used by these other organisms to evaluate environmental signals and regulate their development.

REFERENCES AND NOTES

1. S. Brenner, *Genetics* 77, 71 (1974).
2. R. C. Cassada and R. L. Russell, *Dev. Biol.* **46**, 326 (1975).
3. J. W. Golden and D. L. Riddle, *ibid.* **102**, 368 (1984).
4. ———, *Proc. Natl. Acad. Sci. U.S.A.* **81**, 819 (1984).
5. ———, *J. Chem. Ecol.* **10**, 1265 (1984).
6. P. S. Albert, S. J. Brown, D. L. Riddle, *J. Comp. Neurol.* **198**, 435 (1981).
7. L. A. Perkins, E. M. Hedgecock, J. N. Thomson, J. G. Culotti, *Dev. Biol.* **117**, 456 (1986).
8. D. L. Riddle, in *The Nematode* Caenorhabditis elegans, W. B. Wood, Ed. (Cold Spring Harbor Laboratory, Cold Spring Harbor, NY, 1988), pp. 393–412.
9. J. E. Sulston and J. G. White, *Dev. Biol.* **78**, 577 (1980); M. Chalfie and J. Sulston, *ibid.* **82**, 358 (1981); M. Chalfie *et al.*, *J. Neurosci.* **5**, 956 (1985).
10. L. Avery and H. R. Horvitz, *Cell* **51**, 1071 (1987); *Neuron* **3**, 473 (1989).
11. J. G. White, E. Southgate, J. N. Thomson, S. Brenner, *Philos. Trans. R. Soc. London Ser. B* **275**, 327 (1976); D. G. Albertson and J. N. Thomson, *ibid.*, p. 299; J. G. White, E. Southgate, J. N. Thomson, S. Brenner, *ibid.* **314**, 1 (1986).
12. S. Ward, N. Thomson, J. G. White, S. Brenner, *J. Comp. Neurol.* **160**, 313 (1975); R. W. Ware *et al.*, *ibid.* **162**, 71 (1975).
13. Nematodes were grown under standard conditions (*1*). The eight amphid chemosensory cells were visualized by Nomarski microscopy in young animals and identified by several criteria including the abilities of the cells to fill with fluorescein isothiocyanate [E. M. Hedgecock, J. G. Culotti, J. N. Thomson, L. A. Perkins, *Dev. Biol.* **111**, 158 (1985); (*7*)] and their positions [J. E. Sulston, E. Schierenberg, J. G. White, J. N. Thomson, *Dev. Biol.* **100**, 64 (1983); (*11*)]. They were killed with a laser microbeam system (*10*). Detailed descriptions of cell identification and verification will be presented elsewhere (*22*). All operations were performed within 3 hours of hatching, because dauer larva formation can be initiated only within the first larval stage [M. M. Swanson and D. L. Riddle, *Dev. Biol.* **84**, 27 (1981)].

    For experiments assessing dauer recovery, we isolated dauer larvae by treating starved animals with 2% SDS (*2*). Laser operations on the dauer larvae were carried out as described (*9, 10*). After the operations, animals were allowed to recover in 200 μl of S Basal solution (*1*) in a 96-well microtiter dish, with one animal per well. *Escherichia coli* HB101 was added to the microtiter well 12 to 24 hours after surgery. Mock-operated dauer larvae were isolated with SDS and were mounted on a slide with NaN_3 for the same amount of time as the operated animals.
14. Dauer larvae were identified by their dark color, absence of pharyngeal pumping, and appearance of dauer-specific cuticular ridges (alae) visualized by means of Nomarski microscopy (*2, 8*). Additionally, dauer larvae are resistant to SDS treatment, so many candidate animals were tested for survival after treatment with 2% SDS for >10 min.
15. J. W. Golden and D. L. Riddle, *Science* **218**, 578 (1982).
16. D. L. Riddle, M. M. Swanson, P. S. Albert, *Nature* **290**, 668 (1981).
17. Mutant strains included *che-2 (e1033) X* (*20*), *daf-3 (e1376) X, daf-5 (e1386) II, daf-6 (e1377) X, daf-10 (e1387) IV, daf-12 (m20) X, daf-16 (m26) I, daf-17 (m27) I, daf-18 (e1375) IV, daf-20 (m25) X, daf-22 (m130) II* (*16*). Some strains were provided by the *C. elegans* genetic stock center.
18. These laser experiments identify the last point at which a dauer-defective mutant has a highly penetrant defect in dauer formation. Therefore, any mutant defective so that the animal is independent of chemosensory cell function could also have a defect in the chemosensory cells that is masked by the subsequent defect. The *daf-6* gene is probably one such gene, because it affects chemosensory sensilla (*6*) but is functionally independent of chemosensory cell function. In addition, *daf-16* might cause a partial defect at a later step in dauer formation and a strong defect in chemosensory cell function. Thus, several *daf-16* animals became dauer-like larvae after chemosensory cell kills, but did not differentiate fully into dauer larvae (C. I. Bargmann and H. R. Horvitz, unpublished data).
19. J. W. Golden and D. L. Riddle, *Mol. Gen. Genet.* **198**, 534 (1985).
20. J. A. Lewis and J. A. Hodgkin, *J. Comp. Neurol.* **172**, 489 (1977).
21. W. L. Hubbell and M. D. Bownds, *Annu. Rev. Neurosci.* **2**, 17 (1979).
22. C. I. Bargmann and H. R. Horvitz, in preparation.
23. A. J. Buller, J. C. Eccles, R. M. Eccles, *J. Physiol. (London)* **150**, 417 (1960); W. M. Cowan *et al.*, *Science* **225**, 1258 (1984).
24. A. A. Zalewski, *Exp. Neurol.* **24**, 285 (1969).
25. DeF. Mellon and P. J. Stephens, *Nature* **272**, 246 (1978).
26. J. P. Brockes, *Science* **225**, 1280 (1984).
27. J. W. Truman, *J. Comp. Neurol.* **216**, 445 (1983); K.-i. Kimura and J. W. Truman, *J. Neurosci.* **10**, 403 (1990).
28. P. J. Whitfield, in *Modern Parasitology*, F. E. G. Cox, Ed. (Blackwell, Oxford, United Kingdom, 1982), pp. 34–83; L. H. Chappell, *ibid.*, pp. 116–147; A. Maggenti, *General Nematology* (Springer-Verlag, New York, 1981).
29. D. J. Crisp, in *Chemoreception in Marine Organisms*, P. Grant and A. M. Mackie, Eds. (Academic Press, New York, 1974), pp. 177–265.

30. We thank J. Thomas and L. Avery for discussions and unpublished data and L. Avery, J. Brockes, M. Chalfie, M. Finney, E. Jorgensen, and J. Kaplan for comments on this manuscript. Supported by Public Health Service research grant GM24663. H.R.H. is an investigator of the Howard Hughes Medical Institute. C.I.B. is a fellow of the Helen Hay Whitney Foundation.

4 September 1990; accepted 27 November 1990

Failure to Elicit Neuronal Macroscopic Mechanosensitive Currents Anticipated by Single-Channel Studies

CATHERINE E. MORRIS* AND RICHARD HORN

Mechanosensitive channels can be observed in most cell types during single-channel recording and have been implicated in many cellular processes. Potassium-selective single-channel currents, both stretch-activated and stretch-inactivated, can be observed in growth cones and cell bodies of *Lymnaea stagnalis* neurons. Equivalent macroscopic mechanosensitive currents could not, however, be elicited while applying various mechanical stimuli. This discrepancy suggests that single-channel mechanosensitivity is an artifact of patch recording.

MECHANOSENSITIVE (MS) ION channels have been observed with single-channel recording in more than 30 cell types (*1, 2*), including neurons and their growth cones. For dynamic, tension-generating (*3*) structures, it is easy to conceive of a physiological role for these MS channels, yet direct evidence of a mechanical function for MS channels in growth cones (*4, 5*) or elsewhere is lacking. Mechanotransducing sites in specialized receptor cells remain inaccessible to patch electrodes (*1, 2*). Although the many reports of MS channels suggest that electromechanical irritability is present in most membranes, the cellular-level or macroscopic MS currents (I_{MS}) corresponding to these single-channel events have not been measured.

Neurons of the mollusk *Lymnaea stagnalis* are especially suitable for studying macroscopic I_{MS}. Molluscan growth cones, dynamic structures by definition, have MS channels (*4, 5*) and respond during outgrowth to mechanical stimuli (*6*). Distinguishing nonspecific I_{MS} carried in channels from nonspecific (nonchannel) leak is problematic, but *Lymnaea* MS channels are K^+-selective, so I_{MS} would reverse at potentials different from those for nonspecific leak (*7*). One can minimize space clamp problems and cytoplasmic disruptions by using isolated growth cones and perforated patch recording (*8*).

Tension in the membrane of stretched cells is neither measurable nor homogeneous. Nevertheless, procedures that, taken to their extreme, rupture membranes must increase tension. Figure 1 illustrates the tension-inducing procedures we used with *Lymnaea* neurons. In the following experiments, bath solution (MedK, Table 1) was spritzed (pressure-ejected, Fig. 1A) onto voltage-clamped isolated growth cones. After we verified fluid flow with visible dye on several growth cones, we routinely substan-

C. E. Morris, Biology Department, University of Ottawa, 30 George Glinski, Ottawa, Ontario, Canada K1N 6N5.
R. Horn, Department of Neurosciences, Roche Institute of Molecular Biology, Nutley, NJ 07110.

*Present address: Neuroscience Unit, Loeb Institute, Ottawa Civic Hospital, Ottawa, Ontario, Canada K1Y 4E9.

tiated low pressure flow by observing moving debris. At pressure that generated high flow rates, the growth cone deformed severely and the membrane was deflected along regions of adhesion to the substratum and to the recording pipette. Further increases in pressure stretched the growth cone membrane so that it ruptured. We measured the spritz-induced current using paired voltage ramps (Fig. 2); the difference current for conditions with and without stimuli (I_{diff}) was considered mechanically induced. A spritz-induced I_{diff} reversing near 0 mV (3 of 14 growth cones) was attributed to a change in nonspecific leak. Usually (8 of 14) I_{diff} was <1 pA at all voltages, but in 3 of 14 growth cones, spritzing reduced the amplitude of a current that reversed close to the K^+ equilibrium potential (E_K). Figure 2B represents the largest K^+-specific MS effect observed—a reduction of ≤4 pA, not hundreds of picoamperes of change as expected (*9*) from single-channel data on stretch-activated (SA) and stretch-inactivated (SI) K^+ channels. These experiments provided no evidence of SA K^+ channel involvement (*10*), but inactivation of several SI K^+ channels could explain Fig. 2B.

In the cell-attached configuration (*11*) SA single channels activate during hypo-osmotic shock to an extent that should generate hundreds of picoamperes over a small cell. The whole-cell clamp configuration is unsuitable for osmotic experiments, but we found that hypo-osmotic shock (Table 1) of isolated growth cones in the perforated-patch configuration induced swelling to the point of lysis (Fig. 1B). In spite of the extreme mechanical stimulus associated with osmotic swelling, the K^+ current did not change (six isolated growth cones; repeated steps between −50 mV and −75 mV or voltage ramps as above were used).

The absence of I_{MS} cannot reasonably be attributed to use of the perforated patch method because robust voltage-dependent macroscopic currents could be detected in isolated growth cones (*12*) (Fig. 3). Nor were MS channels disabled in some unanticipated way by growth cone isolation or nonphysiological bath solutions. Cell-attached patches on these isolated growth cones exhibited single SA K^+ channel activity (Fig. 4) similar to that in intact growth cones in normal saline (*5*); SI K^+ channels were also observed (*13*).

Blowing into yeast cells in the whole-cell configuration yields a small nonspecific I_{MS} (*14*); we tried this approach on *Lymnaea* cells (Fig. 1F). Laplace's law predicts that, for a constant internal pressure, tension in a sphere increases linearly with diameter (d) (*14*). Hence, to maximize conditions for measuring I_{MS}, we used somata, not growth cones. In four somata (with inconsequential neurites), we measured I_{MS} at −30 mV (~E_K for cells in MedK) and at −90 mV, with stepwise increases of pressure until cell rupture occurred (inflation was not evident before rupture). No change of holding current occurred at −30 mV. At −90 mV an effect was observed in two cells just below their lytic pressure. In one (d = 45 μm), 70 mmHg caused 7 pA of inward current, and, in the other (d = 30 μm), 20 mmHg in-

Table 1. Recording solutions (millimolar). N, normal; HiK, high K^+ concentration; MedK, medium K^+ concentration; WCR, whole-cell recording; PPR, perforated patch recording. Preshock and shock saline were identical except that 72 mM sucrose was included in the former. pH was adjusted as indicated with 1 N NaOH or KOH: N, pH = 7.6 (Na); HiK, pH = 7.6 (K); MedK, pH = 7.6 (Na-K); WCR, pH = 7.2 (K); PPR, pH = 7.2 (K); shock, pH = 7.6 (K).

Component	N	HiK	MedK	WCR	PPR	Shock
NaCl	50		35.5			
KCl	1.6	51.6	16.6	51.6	10	15.5
$MgCl_2$	2	2	2	2	2	2
$CaCl_2$	3.5	3.5	3.5			3.5
Glucose	5	5	5			5
Hepes	5	5	5	5	5	5
K_2SO_4					35	

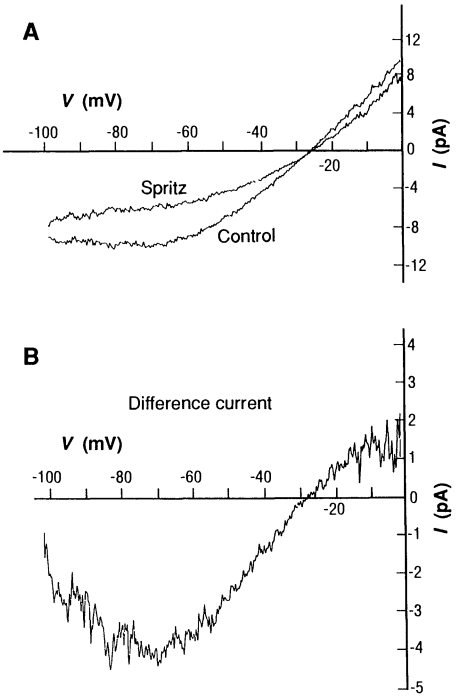

Fig. 2. Macroscopic currents during ramp clamp of an isolated growth cone. R_{series}, 24 megohms; membrane capacitance (C_m), 2.9 pF; holding potential, 0 mV [to inactivate K^+ A currents (*26*)]; ramp of 0 mV to −100 mV over 10 s, 20 s between ramps; cytochalasin-treated growth cone (*10*) in MedK saline. (**A**) Current-voltage relations for ramps without (control) and with (spritz) mechanostimulation. The spritz-induced decrease in K^+ current is evident in (**B**); I_{diff} reverses near E_K (calculated as −27 mV, assuming an activity coefficient of 0.43 for K_2SO_4). A subsequent control (not shown) was indistinguishable from the first; the next pressure increment (12%) destroyed the growth cone.

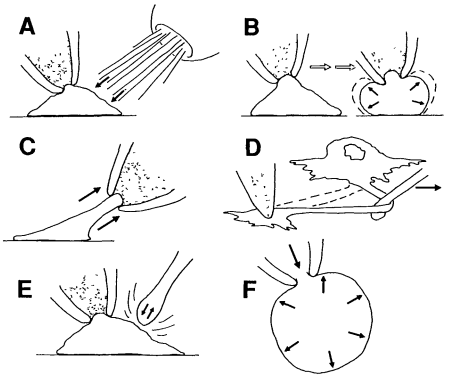

Fig. 1. Modes of mechanical stimulation. Shading indicates the perforated patch configuration; solid arrows, forces or movement; open arrows, the passage of time. (**A**) Spritzing of bath solution on isolated growth cone. (**B**) Hypo-osmotically induced swelling. (**C**) Stretching of the growth cone induced by pulling between the anchor points at the substratum and the gigaohm seal. (**D**) Stretching the neurite while recording at the growth cone. (**E**) Prodding a growth cone with a glass prod. (**F**) Applying pressure by blowing into the soma in the whole-cell configuration. Neurons from circumesophageal ganglia were grown 2 to 4 days on glass or plastic (*5*). Rotund, firmly attached growth cones were severed with a pipette. Procedures, viewed with a Zeiss IM35 microscope (Hoffmann Modulation Optics, Greenvale, New York; ×40 objective), were carried out at room temperature. Four configurations were used: cell-attached patches, outside-out patches, whole-cell, and perforated patch recording. Technical details are given in (*8*). Pipettes (Sylgard-coated, fire-polished borosilicate glass; resistance, ~5 to 10 megohms in *Lymnaea* solutions) yielded gigaohm seals with mild suction. Perforated patch pipettes were filled (*8*) with PPR (Table 1) containing nystatin (160 μg ml^{-1}); in 34 isolated growth cones, the mean ± SD of series resistance (R_{series}) was 25.1 ± 9.5 megohms. For spritzing, a Picospritzer (General Valve, Farfield, New Jersey) was attached to a large (~50 μm) micromanipulator-controlled pipette. To generate and control pressure, we attached a calibrated transducer (Bio-Tek Instruments DPM-1) to the recording pipette.

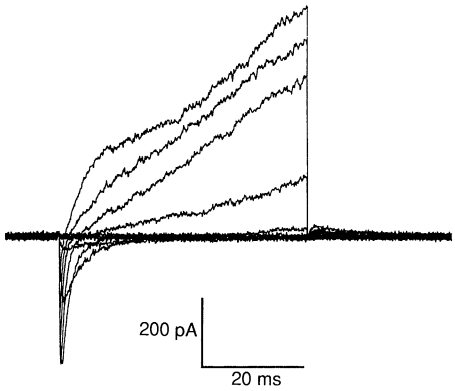

Fig. 3. Macroscopic current of voltage-dependent channels in an isolated growth cone by perforated patch recording. Bath, normal saline; holding potential, −50 mV; R_{series}, 9 megohms; C_m, 3.5 pF; ten depolarizing steps (10-mV increments) applied at 5-s intervals; 80% R_{series} compensation; representative of five growth cones under these conditions (*12*).

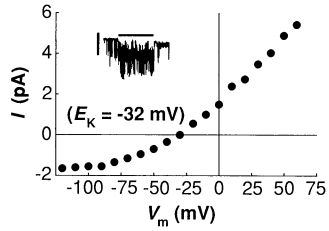

Fig. 4. Single-channel current membrane potential (V_m) relation of SA K^+ channels in a cell-attached patch of an isolated growth cone. Resting membrane potential, 0 mV [HiK in bath (Table 1)]; pipette, MedK. The reversal potential for SA K^+ (and hence any K^+-selective) channels was about −30 mV. (Inset) Single-channel currents after suction (70 mmHg) was applied for 6 s (bar) at −80 mV. Vertical scale, 1.5 pA. Similar results were obtained on five isolated growth cones with these solutions.

duced a current of 6 pA; in either cell these currents correspond to the opening of <4 SA K^+ channels. These cells should (judging their areas from their capacitances and assuming 1 pF ≡ 100 μm^2) have had ≥3400 SA K^+ channels, so the open probability (P_{open}) increased <0.001. Thus, near lytic tension induced negligible macroscopic I_{MS}.

Applying pressure to the inner membrane face of the cell during the whole-cell clamp procedure resembles blowing into an outside-out patch, a stimulus that activates SA channels of *Lymnaea* somata and other preparations (*2, 15*). In agreement with the results from cell-attached patches from isolated growth cones, SA K^+ channels in an outside-out patch from an isolated growth cone were activated at ~50 mmHg. All patch configurations [cell-attached, inside-out (*15*), outside-out] are, therefore, strikingly more stretch-sensitive than whole membrane of *Lymnaea* somata or growth cones, as analyzed by whole-cell or perforated patch voltage clamping.

Prodding molluscan growth cones modifies their outgrowth (*6*); however, prodding isolated growth cones while monitoring for K^+ current with the perforated-patch technique (Fig. 1E) yielded either no change or merely damage-related increases in nonselective leak. Likewise, if the neurite between the growth cone and soma (both attached to the substrate) was stretched (deflected by a glass prod) (Fig. 1D), no effect on macroscopic K^+ current occurred under neurite tensions sufficient to tear the growth cone off the substrate. In addition, no I_{MS} was observed when an electrode attached to a growth cone was slowly pulled back (Fig. 1C), even when the tension tore the growth cone off the substrate. Thus, neither of the stimuli that mimics growth conditions—prodding (*6*) and pulling (*3*)—affected I_{MS} in growth cones (*16*).

Considering Laplace's law and the curvature of cells versus the curvature of patches, pressures smaller than those required in patches should yield cell tensions sufficient to gate I_{MS}. In yeast, pressure did induce I_{MS} in accord with Laplace's law (*14*). Yeast, however, is only slightly larger than outside-out patches and requires "vigorous" suction (*17*) for seal formation. Perhaps only channels near the pipette-membrane seal carry the current; on the basis of yeast channel density (*14*), we calculate that the maximum I_{MS} (at −60 mV) corresponds to recruitment of <2% of the population. Another consideration is the nonselectivity of the yeast MS channels; the graph of I_{MS} plotted as a function of pressure is a nonsaturating curve, a result (*18*) consistent with I_{MS} being carried by a mechanically induced leak through nonchannel pathways.

An ion-selective I_{MS} has been reported (*19*), a shear-activated K^+ current. It was, however, undetectable at the single-channel level. Macroscopic and single-channel mechanosensitive currents have been observed in crayfish stretch receptors (*20*), but the evidence is insufficient to establish whether the single-channel events underlie the I_{MS} (*1*).

The simplest explanation of our data is that *Lymnaea* neurons have two types of K^+-channels (SI and SA) that become hypersensitive to mechanical perturbations only when the membrane-cytoplasm interface is disrupted by gigaohm seal formation. Sachs (*2*) has suggested that the mechanosensitivity of ion channels stems from their linkage to cortical cytoskeletal elements. Alteration of these elements may be required before the channels can be gated by mechanical stimuli (*21*). The existence of ion channels identified as MS by their single-channel behavior is not in doubt, but the nature and relevance of their mechanosensitivity is not clear. Mechanosensitivity may arise as an artifact of patch recording (*22*) in channels that normally are regulated by other agents, for example, second messengers (*1, 23*). This raises concerns about other patch-induced alterations of channel properties.

Speculations about roles for MS channels (*2*) have seemed particularly compelling where single MS channel activity coincides with a relevant physiological process: SA channels in fish oocytes that activate cyclically during cytokinesis (*24*) and other channels that turn on during hypo-osmotic swelling (*11*). If, however, these channels are abnormally mechanosensitive in cell-attached patches, their activation becomes less remarkable. Evidence from healthy cells of appropriate I_{MS} is needed to support the notion that the channels are physiological mechanotransducers. The finding that dystrophic muscle cells (with a cortical cytoskeleton that lacks normal dystrophin) have "leaky" SI channels (*25*) fits the picture of disrupted membranes exhibiting abnormal mechanosensitivity. It is possible that nonpathological alterations of the cortical cytoskeleton in particularly labile membranes (for example, in filopodia or presynaptic terminals) may yet be shown to render otherwise refractory channels mechanosensitive.

Note added in proof: Milton and Caldwell conclude that gigaohm seals disrupt cortical cytoskelton (*27*).

REFERENCES AND NOTES

1. C. E. Morris, *J. Membr. Biol.* **113**, 93 (1990).
2. F. Sachs, in *Cell Shape: Determinants, Regulation and Regulatory Role*, W. D. Stein and F. Bronner, Eds. (Academic Press, New York, 1989), pp. 63–92.
3. P. Lamoreux, R. E. Buxbaum, S. R. Heidemann, *Nature* **340**, 159 (1989).
4. C. E. Morris and W. J. Sigurdson, *Science* **243**, 807 (1989).
5. W. J. Sigurdson and C. E. Morris, *J. Neurosci.* **9**, 2801 (1989).
6. L. R. Mills, M. Murrain, P. Guthrie, S. Kater, *Neurosci. Soc. Abstr.* **14**, 583 (1988).
7. A slightly elevated bath K^+ concentration (MedK, Table 1) provided a nonzero E_K and a sufficient external K^+ concentration for inward K^+ current at potentials negative relative to E_K, where interference from voltage-gated K^+ channels is minimal.
8. S. Korn and R. Horn, *J. Gen. Physiol.* **94**, 789 (1989).
9. If each SI K^+ channel has a conductance of 16.6 pS in MedK (see *4*), 2.6 pA at −50 mV corresponds to ~7 SI K^+ channels. If I_{diff} is due to SI channels at a density of ~1 μm^{-2} (*4*), the spritz reduced the low P_{open} from 0.058 to 0.034. Low P_{open} is consistent with the typically high resistance of isolated growth cones (generally >10 gigaohms) and indicates negligible resting activation of MS channels.
10. Cytochalasin depolymerizes actin [S. J. Smith, *Science* **242**, 708 (1988)] and may enhance SA channel mechanosensitivity [F. Guharay and F. Sachs, *J. Physiol. (London)* **352**, 685 (1984)]. Treating 8 of the 14 growth cones (≥30 min in 10^{-5} M cytochalasin B in 1% dimethyl sulfoxide) resulted in no significant change in MS K^+ currents.
11. C. Bear, *Am. J. Physiol.* **258**, C421 (1990); L. C.

Falke and S. Misler, *Proc. Natl. Acad. Sci. U.S.A.* **86**, 3919 (1989); H. Sackin, *ibid.*, p. 1731; J. Ubl, H. Murer, H.-A. Kolb, *J. Membr. Biol.* **104**, 223 (1988).
12. Isolated growth cones from the heterogeneous cell population had a variable mix of voltage-gated channels. Appropriate solutions and clamp protocols revealed A currents (*26*), voltage-gated Ba^{2+} currents, and those currents illustrated in Fig. 3.
13. Suction of ≥−40 mmHg generally activated SA K^+ channels. SI K^+ channel events were seen in isolated growth cone patches with HiK in the pipette (low conductance in MedK prevents the resolution of SI K^+ channel currents, but SI patch noise was evident).
14. M. C. Gustin *et al.*, *Science* **242**, 762 (1988).
15. W. J. Sigurdson, thesis, University of Ottawa (1990).
16. Lack of resolution was not the problem. On the basis of its capacitance, the isolated growth cone membrane area was 950 ± 440 μm^2 (37 growth cones, median ± SD); an SA K^+ channel density of ~1 μm^{-2} (*5*) would be consistent with a small growth cone having ~500 channels. Under our conditions [single-channel SA K^+ current, ~0.7 pA at −50 mV (Fig. 4)], a stimulus that increased P_{open} to only 0.2 would generate a macroscopic SA K^+ channel current of ~70 pA, more than ten times our level of resolution (Fig. 2).
17. M. C. Gustin, B. Martinac, Y. Saimi, M. R. Culbertson, C. Kung, *Science* **233**, 1195 (1986).
18. Higher pressures were evidently lytic or caused rapid adaptation.
19. S.-P. Olesen *et al.*, *Nature* **331**, 168 (1988).
20. C. Erxleben, *J. Gen. Physiol.* **94**, 1071 (1989); C. Edwards, D. Ottoson, B. Ridqvist, C. Swerup, *Neuroscience* **6**, 1455 (1981).
21. In GH_3 cells (*8*), we observed I_{MS} after disruption of the membrane-cytoplasm interface; whole-cell I_{MS} was elicited reversibly at ≥3 mmHg once pressure had irreversibly distended (presumably, unfolded) the membrane. For a fixed C_m, the diameter increased ~1.5-fold; cells burst at ~10 mmHg without saturation of the I_{MS} versus pressure curve; I_{MS} density was ≥ 0.5 pA μm^{-2} (−70 mV) in each of five cells. In outside-out patches, single-channel events of ~1.2 pA (−70 mV; same solutions) were activated at ~40 mmHg.
22. Another example: the voltage at which inactivation of Na^+ channels occurs shifts in cell-attached patches [T. Kimitsuki, T. Mitsuiye, A. Noma, *Am. J. Physiol.* **258**, H247 (1990)].
23. Serotonin-modulated K^+ channels of *Aplysia* neurons [F. Belardetti, E. Kandel, S. Siegelbaum, *Nature* **325**, 153 (1987)] resemble *Lymnaea* SA K^+ channels and are stretch-sensitive (D. Vandorpe and C. E. Morris, unpublished observations).
24. I. R. Medina and P. D. Bregestovski, *Proc. R. Soc. London Ser. B* **235**, 95 (1988).
25. A. Franco, Jr., and J. B. Lansman, *Nature* **344**, 670 (1990).
26. J. A. Connor and C. F. Stevens, *J. Physiol. (London)* **213**, 21 (1971).
27. R. L. Milton and J. H. Caldwell, *Pfluegers Arch.* **416**, 758 (1990).
28. We thank D. Vandorpe for contributing to some experiments and J. Connor, S. Korn, M. Dickinson, and C. Miller for discussing the manuscript. Supported in part by the Natural Sciences and Engineering Research Council of Canada (grant to C.E.M.).

12 September 1990; accepted 16 November 1990

Paths of Information Flow Through Visual Cortex

MARC MIGNARD* AND JOSEPH G. MALPELI†

The main route of information flow in the cerebral cortex is from the middle layers of cortex to upper and lower layers. However, upper layers of the cat primary visual cortex can be directly driven by inputs from secondary visual cortex when activity in middle layers is disrupted. Upper-layer activity can be driven either by middle layers or by direct corticocortical inputs. One consequence of this result is that areas of cortex thought to be carrying out low-order analysis may be able to extract considerable information from higher order areas.

THE CEREBRAL CORTEX CONSISTS OF six layers, knitted by interlaminar connections into narrow, relatively independent vertical columns (*1*). The input-output transformations of the column are thought to be the key to understanding cortical function. Afferents from specific thalamic nuclei supplying sensory cortex terminate predominately in middle layers (primarily layer 4), suggesting that layer 4 is the main input stage of the column and that information flows from layer 4 to upper (1, 2, and 3) and lower (5 and 6) layers. This idea receives support from the anatomical projections of layer 4 cells to upper and lower layers (*2*), from current-source density analysis (*3*), and from the concentration of cells with "simple" receptive fields in layer 4 of primary visual cortex (V1, area 17) (*4*).

Although layer 4 is undoubtedly critical for full columnar function, our earlier studies showed that when normal interlaminar interactions with layer 4 are disrupted, other layers can generate organized outputs (*5*). The lateral geniculate nucleus (LGN), a laminated thalamic structure, is the major relay of retinal information to cortex. In the cat, the dorsal LGN layers (A and A1) provide the main geniculate input to V1, projecting primarily to layer 4 and secondarily to layer 6 (*6*). When layer A, which receives inputs from the contralateral eye, is

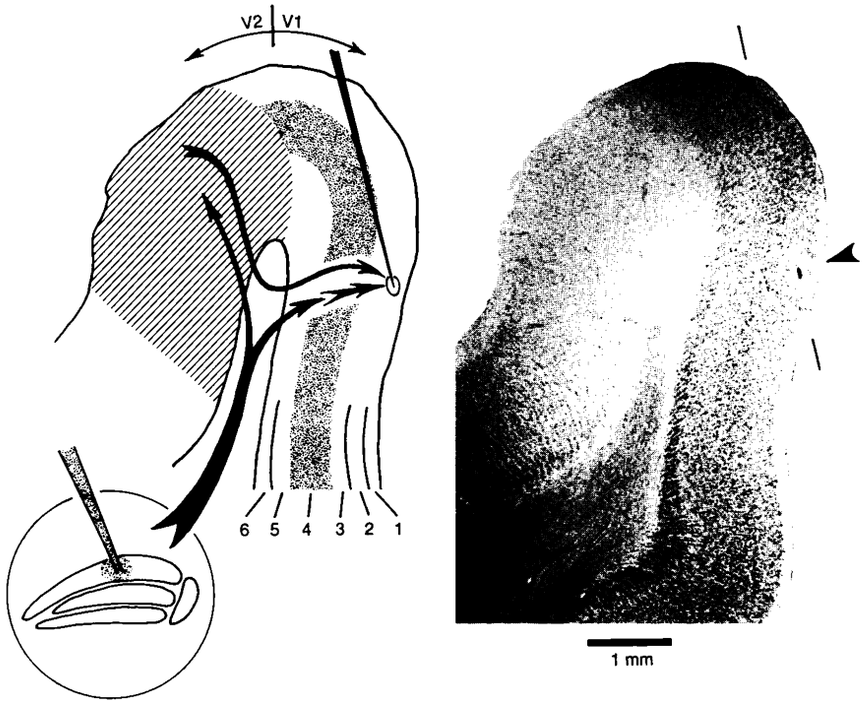

Fig. 1. Main pathways from LGN to upper layers of V1 (left) superimposed on tracing of photomicrograph from actual experiment (right). **Inset:** main LGN subdivisions (layers A, A1, and C, dorsal to ventral; small satellite on right edge is the medial interlaminar nucleus). The lesion in V2 (hatching) was made by injecting 16 mM cobaltous chloride (*18*) through a glass pipette after electrophysiologically mapping the region (460 nl at each of 18 sites in a 3 by 6 grid with 1-mm intersite spacing). The lesion spanned most of the width of V2, extending slightly across the V1-V2 border and 8 mm from anterior to posterior. It corresponded to visual directions from −4° to 16° azimuth and −4° to −17° elevation. Lesions of similar extent were also made with 0.5% ibotenic acid (115 nl at each site in the same grid pattern) (*19*). Entry and exit points of V1 microelectrode (glass-coated tungsten) are indicated by line segments near photomicrograph; arrow, electrolytic marking lesion (*20*).